Intraspinally mediated state-dependent enhancement of motoneurone excitability during fictive scratch in the adult decerebrate cat

Kevin E. Power[1], David A. McCrea[2] and Brent Fedirchuk[2]

[1]*Faculty of Health Sciences, University of Ontario Institute of Technology, Oshawa, Ontario, Canada and* [2]*Department of Physiology, University of Manitoba, Winnipeg, Manitoba, Canada*

This is the first study to report on the increase in motoneurone excitability during fictive scratch in adult decerebrate cats. Intracellular recordings from antidromically identified motoneurones revealed a decrease in the voltage threshold for spike initiation (V_{th}), a suppression of motoneurone afterhyperpolarization and activation of voltage-dependent excitation at the onset of scratch. These state-dependent changes recovered within 10–20 s after scratch and could be evoked after acute transection of the spinal cord at C1. Thus, there is a powerful intraspinal system that can quickly and reversibly re-configure neuronal excitability during spinal network activation. Fictive scratch was evoked in spinal intact and transected decerebrate preparations by stroking the pinnae following topical curare application to the dorsal cervical spinal cord and neuromuscular block. Hyperpolarization of V_{th} occurred (mean −5.8 mV) in about 80% of ipsilateral flexor, extensor or bifunctional motoneurones during fictive scratch. The decrease in V_{th} began before any scratch-evoked motoneurone activity as well as during the initial phase in which extensors are tonically hyperpolarized. The V_{th} of contralateral extensors depolarized by a mean of +3.7 mV during the tonic contralateral extensor activity accompanying ipsilateral scratch. There was a consistent and substantial reduction of afterhyperpolarization amplitude without large increases in motoneurone conductance in both spinal intact and transected preparations. Depolarizing current injection increased, and hyperpolarization decreased the amplitude of rhythmic scratch drive potentials in acute spinal preparations indicating that the spinal scratch-generating network can activate voltage-dependent conductances in motoneurones. The enhanced excitability in spinal preparations associated with fictive scratch indicates the existence of previously unrecognized, intraspinal mechanisms increasing motoneurone excitability.

Abbreviations AHP, afterhyperpolarization; co, contralateral; CP, common peroneal; CPG, central pattern generator; DCC, discontinuous current clamp; EDL, extensor digitorum longus; FDHL, flexor digitorum and hallucis longus; GS, gastrocnemius and soleus; ip, ipsilateral; LGS, lateral gastrocnemius and soleus; MG, medial gastrocnemius; PBSt, posterior biceps and semitendinosus; Plant, plantaris; PLong, peroneous longus; Sart, sartorious; SDP, scratch drive potential; SmAB, semimembranosous; TA, tibialis anterior; Tib, tibial; V_{th}, voltage threshold.

Introduction

Sherrington (1906) referred to motoneurones as the 'final common pathway' to emphasize that independent of complexity of the movement, the nervous system must act through motoneurones to produce the movement. Ultimately, it is the membrane properties of the motoneurone that transform the synaptic drive from descending and sensory systems and from central pattern generators (CPGs) into trains of action potentials during movement. It is now accepted that motoneurone activity results from a complex neuronal integration process involving both passive membrane properties and extrinsically regulated active membrane properties.

Some insight into the role that regulation of motoneurone properties can play in the transformation

of CPG activity into motor output comes from the study of fictive locomotion and scratch in decerebrate adult cat preparations. During fictive locomotion the excitability of lumbar motoneurones is increased through at least three processes. The first is a large hyperpolarization of the action potential voltage threshold (V_{th}) in motoneurones (mean -8 mV; Krawitz *et al.* 2001) that occurs at the onset of fictive locomotion and substantially decreases the amount of synaptic current required to recruit the cell for firing. The second is a depression of motoneurone afterhyperpolarization (AHP) seen during fictive locomotion in adult cats (Brownstone *et al.* 1992) and during pharmacologically induced fictive locomotion in the neonatal *in vitro* rat spinal cord (Schmidt, 1994). This AHP depression probably contributes to the high motoneurone firing rates observed during locomotion (Brownstone *et al.* 1992). The third process increasing motoneurone excitability during fictive locomotion and scratch is the emergence of intrinsic voltage-dependent depolarizations (Brownstone *et al.* 1994). These intrinsic depolarizations can also amplify synaptic input from excitatory reflexes (Lee & Heckman, 2000; Hultborn *et al.* 2003) and further reduce the synaptic drive needed to produce motoneurone firing.

The present study explores changes in motoneurone excitability occurring during fictive scratch. In addition to furthering our understanding of other CPG-generated motoneurone activities, fictive scratch has several advantages over fictive locomotion preparations. Fictive scratch is evoked without brainstem stimulation and thus without the possibility of stimulation-induced effects in motoneurones unrelated to locomotion. Fictive scratch involves rhythmic activity in the ipsilateral hindlimb. On the contralateral side, there is tonic activity in extensors to support the body (Perreault, 2002). Thus, fictive scratch offers the opportunity to examine changes in motoneurone excitability during both rhythmic and postural activities. Fictive scratch can also be evoked in acute spinal preparations and without systemic drug administration (e.g. Sherrington, 1906) to assess whether spinal mechanisms are involved in regulating motoneurone excitability. The present study, therefore, examined changes in motoneurone V_{th}, AHP amplitude, and the emergence of voltage-dependent depolarizations during fictive scratch in both spinal intact and acutely spinalized decerebrate cats.

In the intact animal, scratch consists first of an approach phase in which flexors position the ipsilateral hindlimb near the head. This is followed by a rhythmic phase in which a series of rapid alternating flexion and extension movements scratch the site of irritation, usually the ear. Together these two phases last for a few seconds (Carlson-Kuhta & Smith, 1990). Activity in the contralateral hindlimb may be absent or consist of tonic extensor activity to support the body while the other limb

is scratching. In decerebrate or decapitate preparations scratch can be produced by electrical stimulation of the cervical cord (Sherrington, 1910; Deliagina *et al.* 1975) or by rubbing the ear after topical application of an inhibitory neurotransmitter antagonist such as curare or bicuculline to the cervical spinal cord (Domer & Feldberg, 1960; Degtyarenko *et al.* 1998). Scratch can be evoked in spinal animals (Sherrington, 1906, 1910; Deliagina *et al.* 1981) and in deafferented preparations (Sherrington, 1910; Jankowska, 1959). Scratch-like motoneurone activity can also be evoked following neuromuscular block in decerebrate cats in which case it is termed 'fictive scratch' (Deliagina *et al.* 1975). The occurrence of scratch without afferent feedback and in spinal animals indicates that it results from a spinally located CPG. As in real scratch, activity in the contralateral limb during fictive scratch may be absent or consist of tonic extensor activity during 'fictive weight support' (Perreault, 2002).

There were two broad objectives in the present examination of motoneurone properties during fictive scratch. The first was to determine whether the increases in motoneurone excitability found during fictive locomotion (Krawitz *et al.* 2001) also occur during scratch. Results will show that similar to fictive locomotion, there is a scratch-related hyperpolarization of motoneurone V_{th}, and a reduction of the AHP amplitude that begins at the onset of the approach phase and recovers to control values within a few seconds of the end of scratching. The second objective was to determine whether such state-dependent increases in motoneurone excitability are present in animals acutely spinalized at the C1 level. Results will show that the V_{th} is hyperpolarized, the AHP suppressed and voltage-dependent conductances are activated during fictive scratch in acute spinal preparations. These results provide the first evidence for an intraspinal system that can be recruited by the CPG to facilitate motoneurone excitability in the absence of brainstem stimulation and systemic drug application.

Methods

Data were obtained from 16 cats of either sex. All surgical and experimental protocols were in compliance with the guidelines set out by the Canadian Council for Animal Care and approved by the University of Manitoba Animal Ethics Committee. All three authors have read the article on animal experimentation by Drummond (2009) and confirm that the present experiments comply with the policies and regulations of *The Journal of Physiology*.

Surgical procedures

Anaesthesia was induced and maintained with halothane (1–2%) delivered in an oxygen–nitrous oxide mixture (30%–70%). The level of anaesthesia was monitored by

confirming the absence of pedal withdrawal periodically and by continuously monitoring arterial blood pressure and muscle tone. Cannulae were inserted in the right femoral and jugular veins for drug administration and in the carotid artery for blood pressure monitoring. Atropine (0.05 mg kg^{-1} subcutaneous), saline (10 ml subcutaneous) and dexamethasone (2 mg kg^{-1} intravenous) were given at the beginning of the surgery. A buffer solution (5% glucose, 0.84% bicarbonate solution; 5 ml h^{-1}) was continuously infused through the jugular vein. The bladder was catheterized through the urethra.

Left hindlimb nerves innervating the following muscles were dissected and mounted for recording and stimulation: posterior biceps and semitendinosus (PBSt); semimembranosus and anterior biceps (SmAB); lateral gastrocnemius and soleus (LGS); medial gastrocnemius (MG); gastrocnemius and soleus (GS); plantaris (Plant); tibialis anterior (TA); extensor digitorum longus (EDL); peroneous longus (PLong); flexor digitorum and hallucis longus (FDHL); common peroneal (CP); tibial (Tib); sartorius (Sart). Nerve recordings from the right (contralateral) hindlimb included: TA, Sart and MG (the remaining nerves were cut). The adductor and illiopsoas tendons of both hips were cut.

Following a dorsal laminectomy exposing segments L4 to L7 of the spinal cord, the cat was transferred to a stereotaxic recording frame. The dorsal aspect of the cervical spinal cord was exposed at C1–C2 for topical application of curare to elicit fictive scratch (see below). Mineral oil pools were made for the spinal cord and both hindlimbs, and nerves were placed on conventional silver hook bipolar electrodes for stimulation and recording. The temperature of the animal was maintained by a heating pad and radiant heat lamps. A craniotomy was performed and a precollicular/postmamillary decerebration was completed by blunt dissection and removal of all tissue rostral to the transection. After the decerebration, anaesthesia was discontinued and the animal was neuromuscularly blocked (pancuronium bromide, 0.2 ml supplemented every 45 min) and artificially ventilated. Expired CO_2 was monitored and maintained near 4–5%. Bilateral openings in the chest wall were used to minimize respiratory movements. Decreases in blood pressure were countered by the intravenous administration of a blood volume expander (dextran). At the end of the experiment, animals were given a lethal dose of potassium chloride.

Fictive scratch and weight support

Bouts of fictive scratching and weight support were elicited in the ipsilateral (left) hindlimb by manual stimulation of the left or right pinna, respectively, following topical application of small pieces of curare-soaked cotton (0.1–0.3%) on the left and right C1 and C2 dorsal root entry zones (Domer & Feldberg, 1960). Hindlimb ENG recordings were filtered (30 Hz to 3 kHz), rectified and integrated before digitization at 500 Hz. All signals were captured and analysed using software developed within the Spinal Cord Research Centre and running on a PC in the Linux operating system. Runs of fictive scratch were typically captured in 1 to 3 min segments.

Intracellular recordings

Intracellular recordings (digitized at 10 kHz) were made from antidromically identified lumbar motoneurones using 2 M potassium citrate-filled glass electrodes (tip size 1.6–1.9 μm) to assess V_{th} and AHP. To assess voltage-dependent excitation during fictive scratch, action potentials were blocked by using electrodes filled with the lidocaine derivative QX314 (50 mM) in 2 M potassium acetate. Use of the discontinuous current clamp (DCC) mode of an Axoclamp 2A amplifier (Axon Instruments) permitted reliable measurements of membrane potential during injection of large intracellular currents. The ability of the electrode to pass the current was continuously assessed using a high speed, high gain, oscilloscope trace of the electrode voltage. Under control conditions without fictive scratch, ramp-shaped or rectangular pulses of depolarizing current injection were used to evoke action potentials in the motoneurone. Fictive scratch was initiated later in the same trial, and the intracellular current injection was repeated. The extracellular DC potential recorded immediately after withdrawing the microelectrode was measured and subtracted from the intracellular potential. Recordings in which the intracellular DC values were suspected of drifting were discarded.

Voltage threshold measurement

All reported threshold measurements are for the first spike evoked either by current injection or the first spike occurring on a scratch-induced depolarization. Action potential thresholds were measured under control conditions using depolarizing current ramps (1–2 s duration) or more commonly, depolarizing rectangular pulses (10–20 ms duration). V_{th} was defined as the membrane potential at which depolarization increased at ≥ 10 V s^{-1}. Thus, at the 10 kHz digitization rate used throughout the present study, V_{th} was defined as the value of the membrane potential of the data point that was ≥ 1 mV more depolarized than the preceding point. Figure 1 shows an action potential, its derivative and the current pulse used to evoke the spike. The V_{th} of -43.6 mV is the data point where the derivative trace exceeded ≥ 10 V s^{-1}. This definition of V_{th} was also used during studies on motoneurone threshold changes during fictive locomotion (Krawitz et al. 2001).

V_{th} was measured during fictive scratch from spikes generated by current injection or occurring spontaneously during the depolarizing phase of scratch. Comparisons between values obtained during control and scratch were made using a variety of protocols. In extensors, the V_{th} of the first spike evoked by ramp current injections during control was compared to the V_{th} of the first spike evoked by a ramp during the initial (approach) phase of the scratch in which extensor motoneurones are hyperpolarized. This provided comparisons of both the V_{th} and the threshold current. In other trials, the threshold of the first spike evoked by suprathreshold current pulses just prior to a scratch bout was compared to that of the first current-evoked spike during the hyperpolarized phase of rhythmic scratch activity. These threshold values were also compared to the V_{th} of the first spike evoked spontaneously by scratch-induced depolarizations. As current pulse amplitude was often changed throughout the bout of scratch to ensure spiking during the hyperpolarized phases, threshold current values are not reported for current pulse-evoked spikes.

In all cases, each cell served as its own control using values obtained before and during fictive scratch and usually within 30 s of each other. Changes in $V_{th} < 1$ mV were classified as 'no change.' In most motoneurones three to four measurements were made of first spike V_{th} values and a mean was calculated for each cell. Group mean V_{th} values were calculated using the mean values of individual cells. Unless otherwise stated, all comparisons were tested for statistical significance using a paired *t* test.

Comparisons of V_{th} measurements were made for spikes evoked by ramp and rectangular current injection under control conditions in 10 motoneurones. In nine cells, the V_{th} of current ramp-evoked action potentials was more depolarized (mean $+3.8 \pm 3.6$ mV than the V_{th}

obtained using a current pulse (Wilcoxon signed rank test; $P = 0.04$). This difference was probably due to an accommodation of voltage-gated sodium channels caused by the relatively slow rate of rise of the depolarizing ramps (e.g. Kuo *et al.* 2006). Consequently we do not report comparisons of V_{th} of ramp-evoked control spikes and spikes evoked by pulses or spikes occurring spontaneously during scratch. Comparisons are reported for the V_{th} of spikes evoked by current pulses with those occurring spontaneously on scratch cycle depolarizations (scratch drive potentials, SDPs; Degtyarenko *et al.* 1998).

Afterhyperpolarization assessment

Ramp current injections and suprathreshold 0.5 ms current pulses were used to evoke action potentials and examine motoneurone AHPs in control conditions and during fictive scratch. Quantitative measures of AHP amplitude were made difficult by the lack of an appropriate baseline from which to measure the peak amplitude of the AHP. Thus, the present report provides only a qualitative comparison of the depression of AHP amplitude that occurs during scratch activity.

Conductance measurements

Averaged peak voltage deflections resulting from a 5 nA, 4–5 ms hyperpolarizing current pulse were used to assess changes in input resistance between control and fictive scratch conditions. The voltage responses occurring during the tonic and rhythmic phases were averaged separately. Pulses occurring immediately following a spike were not averaged to avoid potential contamination with the activation of voltage-gated conductances. The
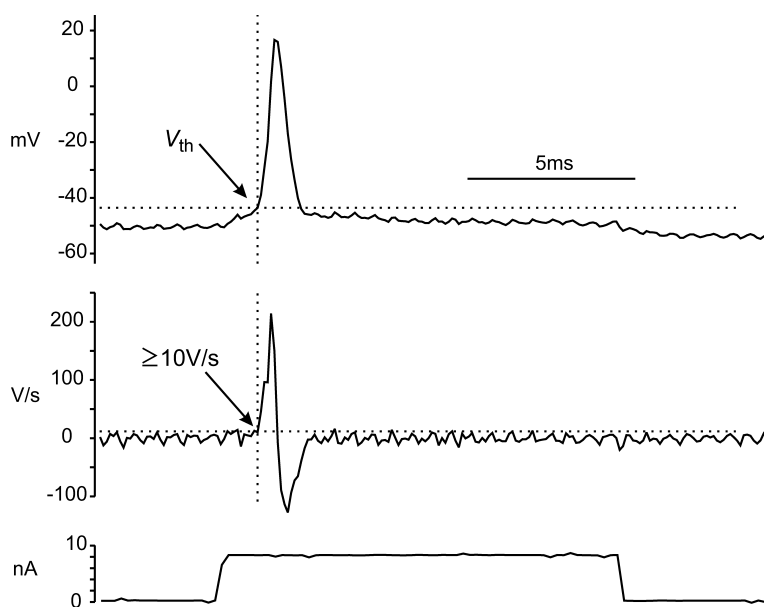

Figure 1. Method of V_{th} determination
Upper trace: intracellular recording from an extensor motoneurone in the SmAB motor pool in discontinuous current clamp mode (10 kHz switching) and digitized at 10 kHz. The voltage threshold of the action potential (V_{th}) evoked by a rectangular current pulse (lower trace) was defined as the data point at which the change in membrane potential of subsequent points exceeds 1 mV (indicated by the arrow). Middle trace: the derivative of the intracellular trace shows that the V_{th} data point clearly corresponds to the fast rising portion of the spike where the voltage trajectory surpasses 10 V s^{-1}. The oscillating noise on the traces is the result of switching artifacts from the discontinuous current clamp.

estimated conductance was then obtained by dividing the amplitude of the current injected during the pulse by the ensuing peak voltage deflection.

Scratch drive potential (SDP) amplitude measurement

To observe SDP amplitudes during fictive scratch it was necessary to block action potentials with the lidocaine derivative QX314 (50 mM) added to the recording micro-electrode. During bouts of fictive scratch, recordings were made with and without constant or ramp current injection to examine any voltage-dependent behaviour. SDP amplitude was defined as the maximum, peak-to-peak value obtained by measuring the membrane potential at the base of the hyperpolarising trough of the SDP and the peak depolarization of the SDP.

Acute spinalization

In seven cats an acute complete transection of the spinal cord was made at C1 to eliminate descending input to the spinal cord. Transection was carried out using pairs of fine forceps and applying small pieces of cotton soaked in lidocaine to the spinal cord. Fictive scratch and motoneurone properties in the spinalized preparations were examined before and after transection. Two of these animals were used only for V_{th} measurements and five were used to examine voltage-dependent amplification of centrally generated depolarizations during fictive scratch.

Results

The V_{th}, AHP amplitude and the presence of voltage-dependent increases in the amplitude of the SDP were assessed in antidromically identified motoneurones innervating a variety of hindlimb flexor, extensor and bifunctional motoneurones in 16 adult, decerebrate cats. Fictive scratch was evoked by manual manipulation of the ipsilateral ear following curare application to the dorsal surface of the cervical cord. Data are reported only from those motoneurones with action potential amplitudes ≥ 60 mV and without obvious changes in action potential shape, amplitude or duration during or after a bout of fictive scratch. The large range of rheobase currents (3–25 nA) recorded under control conditions suggests that motoneurones innervating both slow (low rheobase) and fast (high rheobase) twitch muscle fibres were included in the sample (Zengel *et al.* 1985; Hochman & McCrea, 1994). The principal finding is that there is a state-dependent increase in motoneurone excitability during fictive scratch that continues to be recruited following acute spinal trans-ection.

V_{th} hyperpolarization in spinal intact cats

Figure 2*A* and *B* shows records of TA (ankle flexor) and GS (ankle extensor) ENGs, an intracellular recording from a GS motoneurone and the current monitor trace. The control records in Fig. 2*A* were obtained about 4 s before the left ear was rubbed to initiate the episode of fictive scratch shown in Fig. 2*B*. The tonic activity in the TA nerve in Fig. 2*B* is the initial approach phase of scratch that precedes rhythmic alternating bursts of activity in flexor (TA) and extensor (GS) motoneurones. Although the duration of the approach phase in Fig. 2 is typical, in other bouts of fictive scratch this phase may be brief or absent and may be preceded by a brief burst in some of the extensors (see the portion of the intracellular trace in Fig. 7*A* at 10 s and in 7*C*).

The TA ENG, intracellular and current monitor traces from the indicated regions in Fig. 2*A and B* are shown on expanded time bases in panels *C*, *D* and *E*. A depolarizing current ramp delivered to the GS motoneurone before the onset of scratch (control, Fig. 2*A* and *C*) evoked an action potential as the current reached 14.6 nA. The V_{th} of this spike was -36.5 mV (Fig. 2*C*). The second current injection began just prior to the onset of the approach phase. As the current reached 9.8 nA an action potential with a V_{th} of -43.9 mV was evoked (Fig. 2*D*). It is important to note that extensor motoneurones are tonically hyperpolarized during the initial period of tonic flexor activity in these preparations (Perreault, 2002). Thus, well before extensor activity, and just prior to flexor activity, the V_{th} in this extensor motoneurone became lower (i.e. hyperpolarized) by 7.4 mV and the spike was evoked by about 1/3 less current. These changes occurred more than 1 s before the onset of extensor motoneurone activity. This lowering of V_{th} during fictive scratch was not accompanied by obvious changes in action potential duration or height. V_{th} was hyper-polarized during the approach phase in all but one of nine extensor motoneurones examined (mean -3.1 ± 1.9 mV, range: -1.8 to -7.4 mV; $P < 0.01$, $n = 9$) by rectangular pulse (2 cells) or current ramp (7 cells) injection in spinal intact cats. Current thresholds of the first spike evoked by ramp current injection decreased from a control mean of 17.8 ± 5.3 nA to 12.8 ± 6.1 nA in the approach phase ($P < 0.05$, $n = 7$). Thus, despite the tonic hyperpolarization of extensor motoneurones during the approach phase, motoneurone excitability was enhanced with a hyperpolarization of V_{th}.

Extensor motoneurones are briefly depolarized and typically fire two to five action potentials during each cycle during the rhythmic portion of scratch. The V_{th} of the first action potential occurring spontaneously on the first SDP in the GS motoneurone in Fig. 2*E* was -46.6 mV. Although this spike begins from an obviously hyperpolarized membrane potential compared

to control (Fig. 2*C*), quantitative comparisons of the V_{th} between ramp-generated and SDP-generated spikes were considered unreliable and are not reported (see Methods). Note the very short (8 ms) first inter-spike interval in Fig. 2*E*. Changes in the AHP during scratch are described further below.

Figure 3*A* shows the GS ENG (top), an intracellular recording of a GS motoneurone during fictive scratch (middle trace) and the current monitor (bottom). Supra-threshold rectangular current pulses delivered at approximately 2 Hz during fictive scratch and at random

with respect to the scratch cycle were used to compare the V_{th} of spikes evoked under control conditions to those evoked during the hyperpolarized phase of the SDP and to those evoked spontaneously by the rhythmic depolarization during scratch. The V_{th} of the control action potential was −39.4 mV (Fig. 3*B*). Current injection during the hyperpolarized portion of the SDP evoked an action potential with a threshold 2.1 mV lower than control (Fig. 3*C*). The threshold current for evoking an action potential during the hyperpolarizing phase of scratch activity was not determined. All seven cells
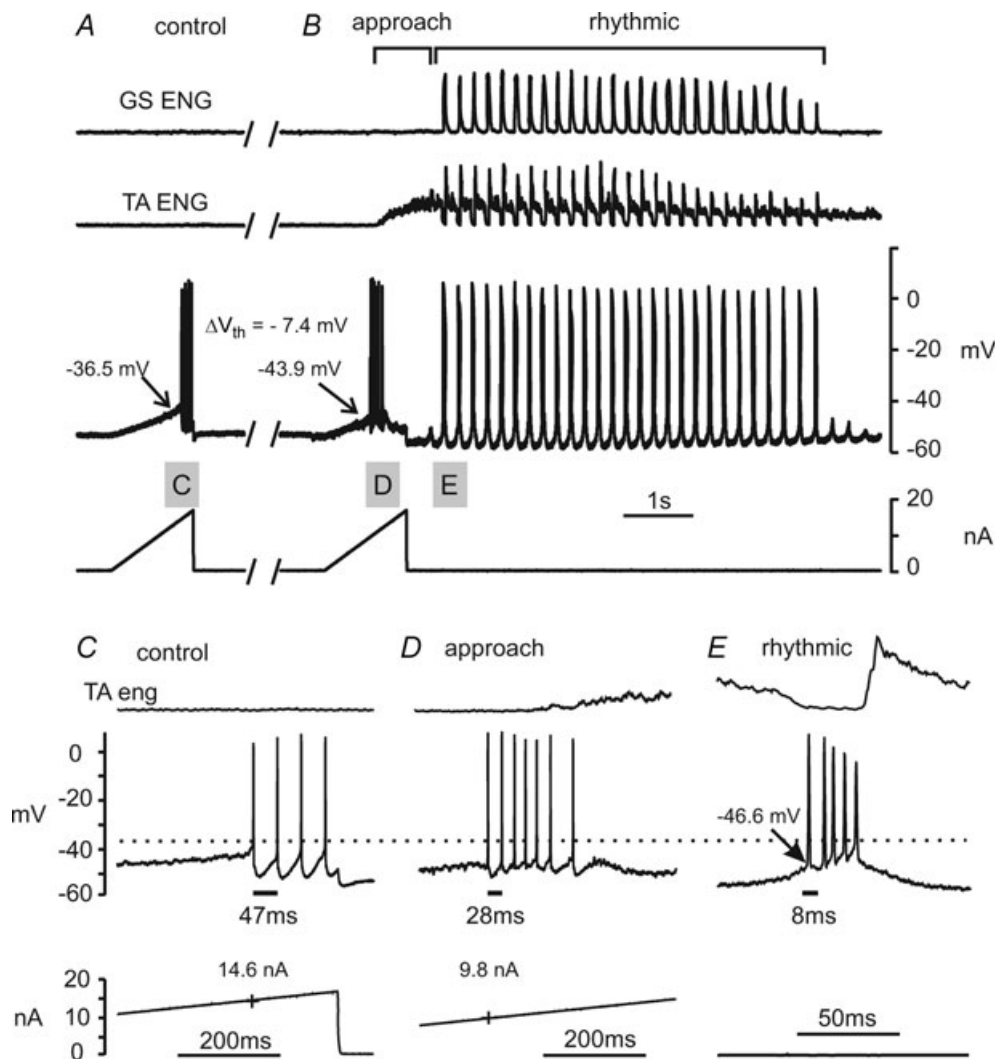

Figure 2. V_{th} is hyperpolarized during fictive scratch
A and *B* show extensor (GS) and flexor (TA) ENG recordings, the intracellular recording from a GS motoneurone and the current monitor trace in a spinal cord intact preparation. Records in *A* taken about 7 s before those in *B* show action potentials evoked under control conditions by a ramp-shaped current injection. The ENG traces in *B* show the approach and rhythmic phases of fictive scratch evoked by rubbing the ipsilateral ear. A portion of the intracellular trace and TA ENG trace (indicated by the shaded boxes) are shown expanded in *C*. Spikes evoked by current injection just prior to the onset of tonic TA ENG activity are shown in *D*. The spikes occurring spontaneously on the first supra-threshold depolarizing SDP during scratch are shown in *E* at a more expanded time base than those in *C* and *D*. The V_{th} of this motoneurone hyperpolarized by −7.4 mV prior to the onset of ENG activity during scratch and remained hyperpolarized during the rhythmic activity associated with the bout of scratch. The duration of the first inter-spike intervals are shown below the firing in panels *C*, *D* and *E*.

examined during the hyperpolarizing phase of the SDP had a V_{th} that was hyperpolarized compared to control (mean hyperpolarization: -4.2 ± 3.0 mV; range: -1.1 to -8.6 mV; $P < 0.05$).

Figure 3C shows that the V_{th} of the spike evoked by current injection during the hyperpolarizing portion of the SDP was similar to that of the first spike appearing on the depolarizing potion of the SDP. Thus, compared to control, V_{th} was hyperpolarized during both the de- and hyperpolarizing phases of the SDP. V_{th} is also hyperpolarized during both fictive locomotor phases (Krawitz *et al.* 2001). During fictive scratch there was a tendency for the V_{th} of the spike evoked during the hyperpolarizing SDP to be more hyperpolarized than the V_{th} of the first spike evoked on the depolarizing SDP (difference 1.8 mV, $P < 0.01$, $n = 6$). The V_{th} values for the two subsequent spikes during the illustrated scratch cycle in Fig. 3C were higher than that of the first, presumably due to accommodation (note the decreased spike amplitude of the thirds spike during the two bursts in Fig. 3A).

V_{th} hyperpolarization in acute spinal cats

In order to determine whether changes in V_{th} can occur after acute interruption of descending input to the cord, motoneurone V_{th} was measured during fictive scratch after complete transection of the spinal cord at the C1 level in two cats. Figure 4 shows the pattern of fictive scratch ENG activity before (Fig. 4A) and after spinal transection

(Fig. 4B) in the same experiment with expanded records in 4C. Note the similarity of ENG activity patterns, cycle periods and phase durations before and after spinalization. In spinal cord-intact preparations PLong activity during scratch begins during the extensor bursts and has a duration similar to that of hindlimb extensors (Deliagina *et al.* 1981; Lafreniere-Roula & McCrea, 2005). The extensor phase activity of PLong contrasts with the flexor phase activity seen during fictive locomotion (see Lafreniere-Roula & McCrea, 2005). The persistence of this extensor-like activity in PLong after spinalization (Fig. 4C) indicates that this pattern is accomplished by circuitry within the spinal cord.

Figure 5 shows an intracellular recording from a MG motoneurone in an acute spinal cat. During control conditions, a supra-threshold current pulse evoked an action potential with a V_{th} of -48.6 mV (Fig. 5B). During scratch, rhythmic depolarizations of the SDP induced one or two action potentials during each scratch cycle (Fig. 5A). The V_{th} of the SDP-induced spike illustrated in Fig. 5C was -53.3 mV, a 4.7 mV hyperpolarization of V_{th} during scratch. The V_{th} of current pulse-evoked spikes was measured in 13 (1 flexor, 8 extensor and 4 PBSt) motoneurones during control conditions in two spinal transected cats and compared to thresholds of action potentials evoked by fictive scratch SDPs (7 motoneurones) or spikes evoked by a depolarizing current pulse on top of a sub-threshold depolarizing SDP (6 cells). With the onset of fictive scratch there was a V_{th}
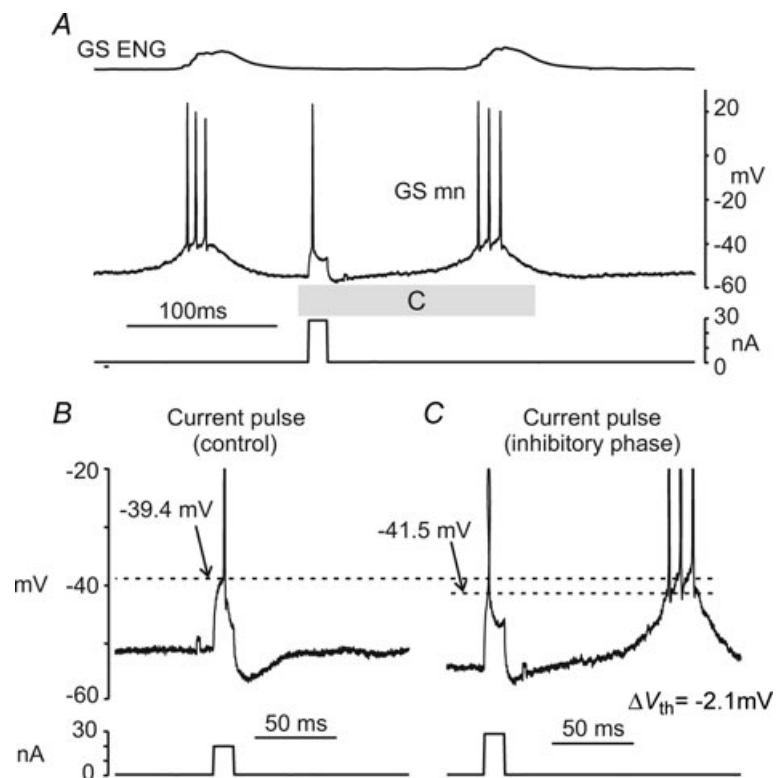

Figure 3. V_{th} is hyperpolarized during the active and inactive portions of the fictive scratch cycle
A shows extensor (GS) ENG activity during ipsilateral fictive scratch (top trace) and the intracellular membrane potential recording and current injection (middle traces) for a GS motoneurone in a preparation with an intact spinal cord. The shaded area denotes the portion illustrated in *C* on an expanded timescale. The V_{th} for action potentials before fictive scratch was -39.4 mV and was elicited by a 19 nA rectangular current pulse. The current was increased to 28 nA to ensure spiking during the hyperpolarized phase of the SDP. *C* shows the thresholds of the current-evoked action potential and the action potential evoked by the SDP were similar and hyperpolarized by -2.1 mV compared to control (*B*). Note the spikes are truncated in panels *B* and *C*.

hyperpolarization in all but one of the 13 cells (mean change: -6.6 ± 7.9 mV, $n = 13$; mean hyperpolarization: -7.1 ± 8.1 mV; range: -1.3 to -26.2 mV; $P < 0.05$, $n = 12$). As was the case in spinal-intact preparations, there were no obvious changes in action potential shape or duration associated with the hyperpolarization of V_{th}.

V_{th} depolarizes during fictive weight support

Fictive weight support involves tonic firing of contralateral hindlimb extensor motoneurones during ipsilateral fictive scratch (Perreault *et al.* 1999). Figure 6 shows a bout of fictive scratch on the ipsilateral side followed a few seconds later by contralateral fictive scratch (see coTA and coMG activities). Portions of the records indicated in *A* are shown on an expanded time base in *B* and *C*. During control conditions, the V_{th} obtained from intracellular current pulses in this SmAB motoneurone was -45.6 mV (lower trace, panel 6*A*). Ipsilateral scratch was then induced by rubbing the left ear of the cat. As can be seen in the expanded time scale of panel *B*, the motoneurone fired three to five spikes on each depolarizing SDP. The average V_{th} of the first action potential occurring on the SDP was -47.4 mV, a hyperpolarization of 1.8 mV. The V_{th} of the motoneurone recovered to -45.7 mV within $\sim$6 s following the rhythmic scratch activity.

Approximately 3–5 s later, the cell had depolarized slightly and the V_{th} was -43.3 mV. The contralateral (right) ear was then rubbed to evoke an episode of scratch on the contralateral side. Contralateral scratch began with tonic (approach phase) activity in the contralateral ankle flexor nerve (coTA) as well as tonic (fictive weight support) activity in ipsilateral extensor motoneurones (ipSmAB) that preceded the alternating activity in contralateral extensors and flexors. As seen in Fig. 6*C*, the V_{th} of the ipsilateral extensor motoneurone rapidly (within 500 ms) depolarized to -40.6 mV and then to -35.4 mV (a change of $+7.9$ mV) as it began to fire fictive weight support. Similar to the hyperpolarization of V_{th} ipsilateral scratch, the depolarization of V_{th} during fictive weight support began before the onset of any scratch-induced firing. The firing frequency was slower (i.e. longer inter-spike intervals) during fictive weight support than during the excitatory phase of the SDP illustrated in Fig. 6*B*. Note also that spike amplitude is maintained during ipsilateral scratch but is reduced during and recovers immediately after, fictive weight support. As judged by the failure of the first current pulse in panel *B* to evoke a spike, current threshold during the hyperpolarized phase of ipsilateral fictive scratch was around 16 nA and was reduced considerably during fictive weight support.

In one cell V_{th} was hyperpolarized by -2.1 mV during fictive body weight support. In the other six extensor cells examined, motoneurone V_{th} depolarized
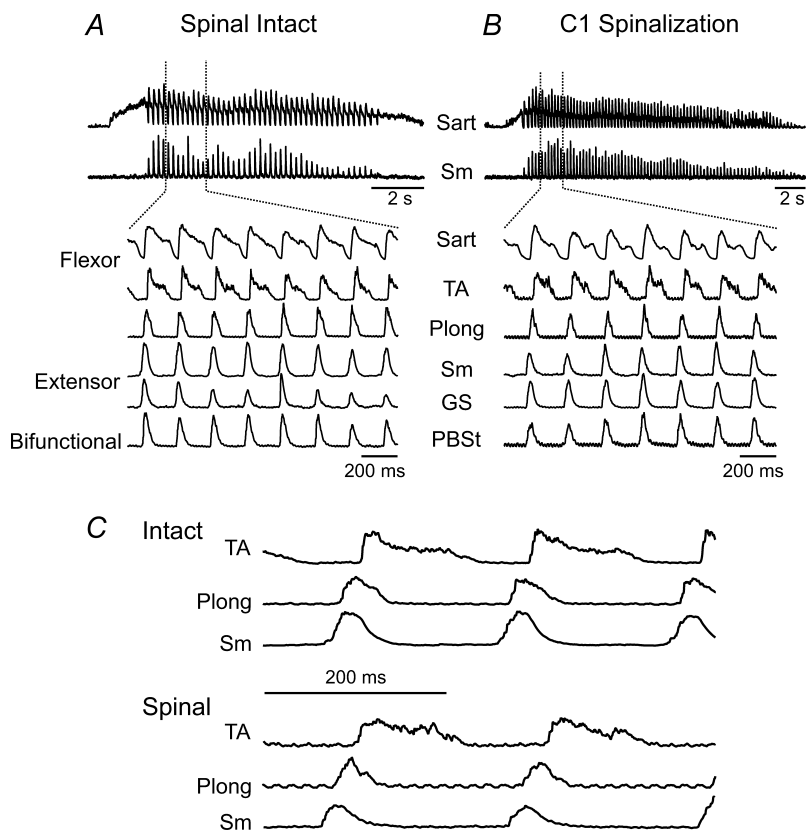

Figure 4. Similar patterns of fictive scratch activity before and after spinal transection
The 2 upper traces in *A* and *B* show episodes of fictive scratch in the same preparation before (*A*) and after (*B*) an acute complete transection of the spinal cord at the C1 level. ENG recordings from other nerves are shown at a faster time base below. The similarity of the pattern of ENG activities, duration of motoneurone pool discharges and cycle periods before and after spinalization are evident in the records in *C*.

during fictive body weight support (mean depolarization: $+3.7 \pm 1.7$ mV; range: $+1.7$ to $+5.9$ mV; $P < 0.05$, $n = 6$). This V_{th} depolarization contrasts with the hyperpolarization occurring routinely during fictive locomotion (Krawitz et al. 2001) and ipsilateral scratch.

Summary of V_{th} changes during fictive scratch

V_{th} was examined in 41 motoneurones in preparations with intact spinal cords during ipsilateral scratch (25 hip or ankle extensors; 5 ankle flexors, 8 PBSt and 3 FDHL motoneurones). The mean change in the V_{th} during scratch when all 41 observations were pooled was -4.2 ± 4.6 mV. In five cells, V_{th} became depolarized by an average of 1.5 ± 1.1 mV during ipsilateral scratch, and in three cells there was no change in threshold. In the cells in which V_{th} hyperpolarized, the mean change was -5.4 ± 4.3 mV (range: -1.1 to -19.8 mV; $P < 0.001$, $n = 33$). V_{th} lowering was seen in flexor (3/5, mean -3.7 ± 1.9 mV) extensor (19/25, mean -5.4 ± 4.6 mV) PBSt (8/8, mean -5.6 ± 4.2 mV) and FDHL (3/3, mean -2.4 ± 2.0 mV) motoneurones. The mean change in spinal-intact preparations (-5.4 ± 4.3 mV, $n = 33$) was not statistically different ($P = 0.38$) from the mean -7.1 ± 1.9 mV hyperpolarization in acute spinal animals described above. Pooling the 41 observations from spinal cord-intact and 13 from transected preparations, the V_{th} of 45/54 (83%) motoneurones was hyperpolarized during ipsilateral fictive scratch (mean -5.8 ± 5.5 mV).

As reflected in the large standard deviations of the population means, there was considerable variability in the degree of threshold lowering between individual motoneurones. The row of numbers below the bar graph in Fig. 8 shows the change in V_{th} in 10 motoneurones from one experiment with the first three obtained before spinal transection. As can be seen, the values varied widely even within a single preparation. The -26.2 mV value in a SmAB motoneurone following spinalization was the largest change encountered in the present study and much larger than the hyperpolarization in two other SmAB motoneurones recorded under the same conditions. Presently, we have no obvious explanation for the large range of V_{th} changes between motoneurones during scratch. In spinal-intact preparations there were no correlations between the magnitude of V_{th} hyperpolarization during fictive scratch and initial membrane potential ($r^2 = 0.17$, $P = 0.35$), rheobase ($r^2 = -0.09$, $P = 0.65$) or SDP amplitude ($r^2 = -0.15$, $P = 0.65$). Similarly, in acute spinal preparations, there were no correlations between the amount of V_{th} hyperpolarization seen during fictive scratch with initial membrane potential ($r^2 = -0.22$, $P = 0.68$), rheobase ($r^2 = -0.12$, $P = 0.82$) or SDP amplitude ($r^2 = 0.25$, $P = 0.69$).

The recovery of V_{th} hyperpolarization following a bout of fictive scratch to control values was followed in 16 cells. In nine, recovery was complete within 10–20 s while in the other seven, V_{th} had only partially returned to control values within 20 s. An example of recovery of threshold hyperpolarization following an episode of fictive scratch is seen in Fig. 6A. The time course of recovery appeared similar in spinal intact and transected preparations.

These observations on V_{th} obtained during ipsilateral fictive scratch are similar to those obtained during mid-brain stimulation-evoked fictive locomotion (Krawitz et al. 2001). The rapid threshold hyperpolarization seen with the onset of fictive scratch in acute spinal preparations is evidence for the operation of an intra-spinal mechanism regulating motoneurone threshold properties.

AHP amplitude is reduced during fictive scratch in the decerebrate cat

Figure 7A shows records from a GS motoneurone in which action potentials were evoked spontaneously by rhythmic scratch depolarizations and by current ramps under control and recovery conditions. Portions of the
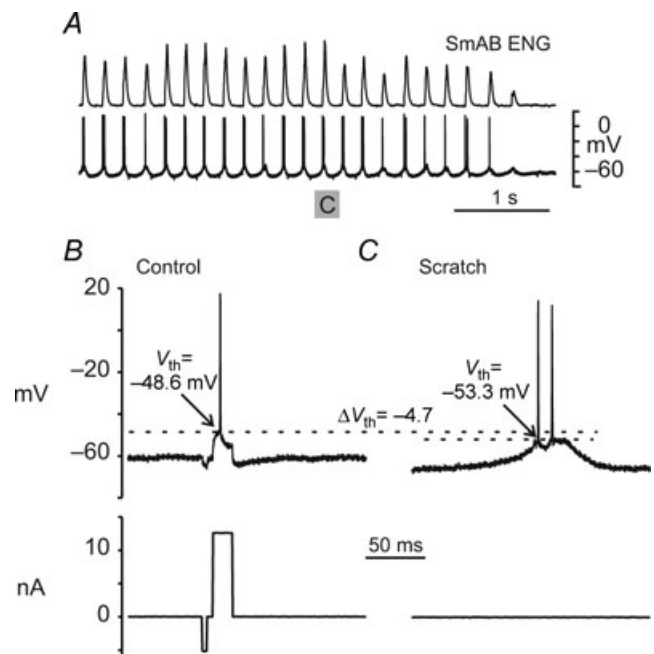

Figure 5. V_{th} is hyperpolarized during fictive scratch after spinal transection
A shows the SmAB ENG and an intracellular recording from a MG motoneurone during the rhythmic portion of an episode of fictive scratch in an acutely spinalized cat. Intracellular and current monitor traces are shown in B and C on an expanded time base. The V_{th} of spikes occurring on the SDP was hyperpolarized by -4.7 mV during scratch (C) compared to those evoked by current injection during control conditions (B). The current monitor trace in B shows the small hyperpolarizing current pulse used to assess membrane conductance.

records in *A* are shown expanded in *B–E*. The action potentials during scratch occur at a membrane potential that is obviously hyperpolarized compared to control (V_{th} −53 mV during scratch; −47 mV in control) but as described in Methods, quantitative comparisons between V_{th} values obtained from ramps and from SDP firing were not considered reliable. Of note in Fig. 7*B* is the prominent AHP following each action potential in control conditions. Immediately prior to the onset of the approach phase, the AHP is attenuated (Fig. 7*C*) becoming almost

undetectable during rhythmic fictive scratch (Fig. 7*E*). Similar to the example in Fig. 2, the interspike interval during scratch becomes very short. As the bout of scratch comes to an end and the SDPs disappear (Fig. 7*D*), AHP amplitude begins to recover. AHP amplitude and the firing rate return to control levels within 10 s after the bout of scratch. This is illustrated in the inset in Fig. 7*B* which shows an overlay of the first three action potentials evoked during control conditions (from panel 7*B*) and 10 s after fictive scratch (*). Figures 2 and 3 show similar
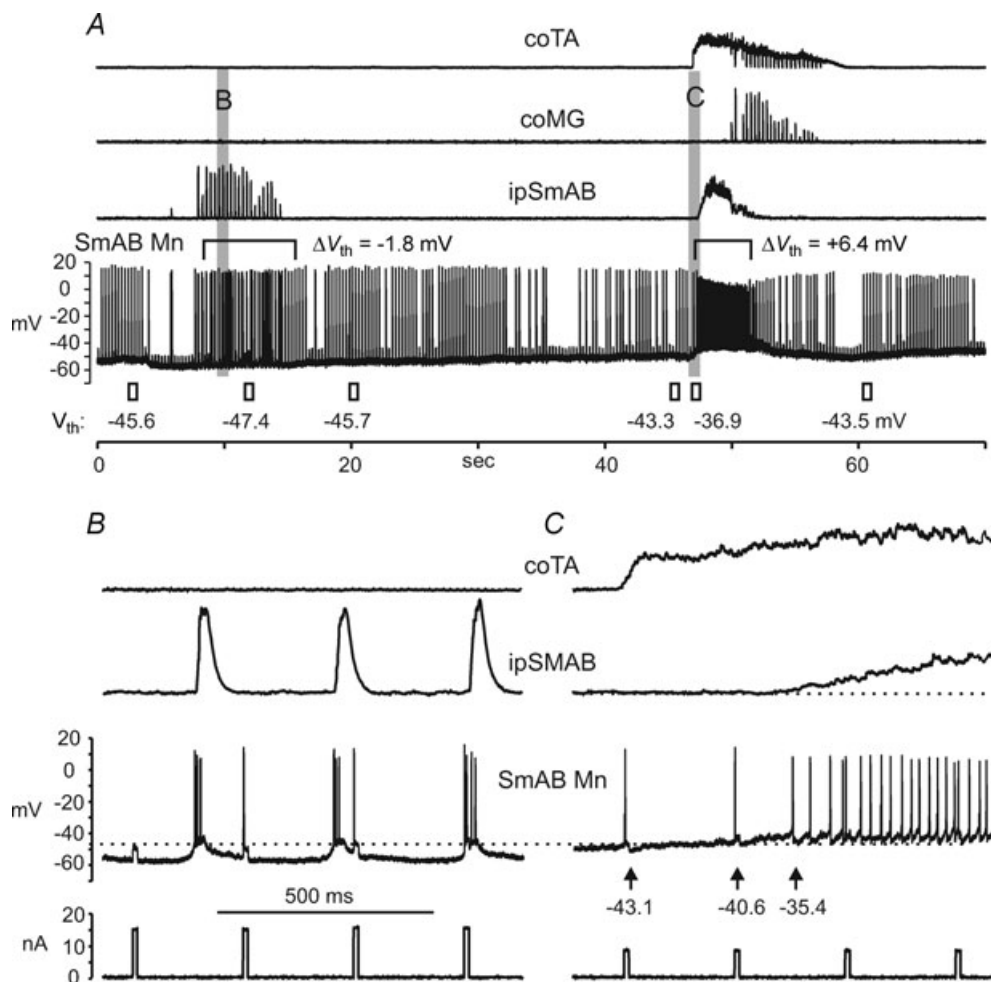

Figure 6. V_{th} is depolarized during fictive weight support and hyperpolarized during ipsilateral scratching
A shows continuous ENG records, first during ipsilateral rhythmic scratching evoked by rubbing the ipsilateral ear (8–15 s in the run), and then during contralateral scratch evoked by rubbing the other ear (48–58 s) in a decerebrate cat without spinal transection. During the approach phase of contralateral scratch (i.e. during tonic activity in the contralateral flexor, coTA) the ipsilateral extensor ipSmAB displays tonic 'fictive weight support' activity (48–52 s). The intracellular record from a SmAB motoneurone is shown below the ENGs, and representative values of the V_{th} measured throughout the run are shown below. Expanded records of the regions indicated by the vertical shaded areas are shown in *B* and *C*. Depolarizing current pulses were delivered throughout the run to evoke firing in addition to the spontaneous, scratch-induced firing. The control V_{th} of −45.6 mV (left-most value) is hyperpolarized by −1.8 mV (to −47.4 mV) during the rhythmic phase of ipsilateral scratch (see *B*) and recovers a few seconds after the end of ipsilateral scratch activity. During the fictive weight support that begins at about 48 s (see *C*), V_{th} depolarized by +6.4 mV from the control value immediately before contralateral scratch began (i.e. from −43.3 to −36.9 mV; see *C* for values from individual spikes).

examples of AHP reduction during fictive scratch. In Fig. 3 there is a large hyperpolarization following the current pulse-evoked spike during control conditions (3*B*) but not scratch (3*C*). Finally, the AHP is almost absent during SDP-evoked firing in Fig. 5. During fictive weight support (i.e. during contralateral scratch) AHP reduction was less pronounced than during ipsilateral scratch (Fig. 6*B* and *C*).

Together, these examples show that the AHP evoked by current pulses, ramp currents or following spontaneous spikes on the SDP is severely reduced during fictive scratch. A quantitative assessment of the magnitude of this AHP reduction is, however, compromised by the lack of an appropriate baseline from which to measure AHP amplitude. Since the V_{th} is hyperpolarized during scratch, choosing the membrane potential immediately preceding
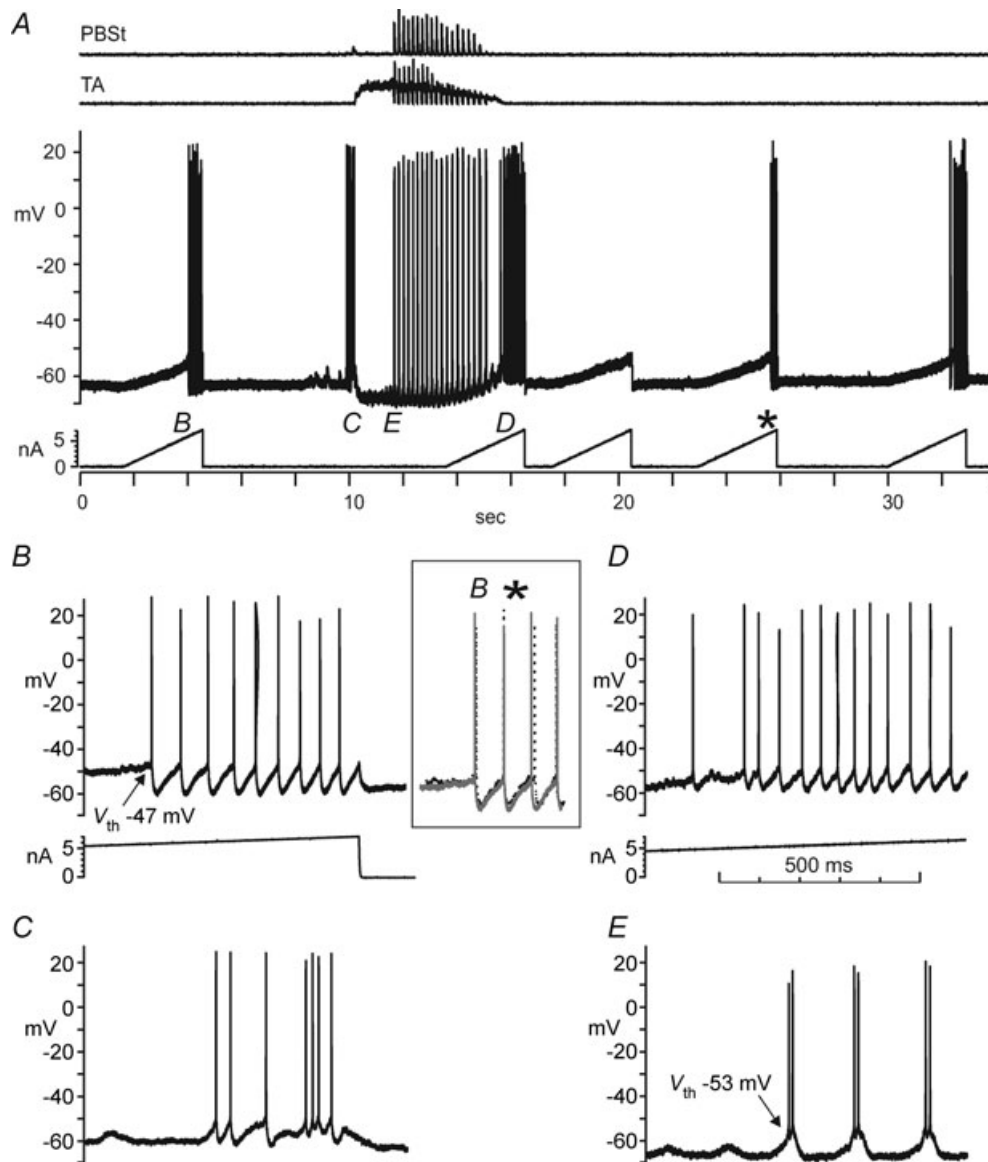

Figure 7. Afterhyperpolarization amplitude is reduced during fictive scratch
A illustrates extensor (PBSt) and flexor (TA) ENG recordings, the intracellular recording from a GS motoneurone and the current monitor trace. Records in *A* labelled *B*, *D* and * show on an expanded timescale, action potentials evoked by ramp-shaped current injection prior to (*B*) and following (*D* and *) ipsilateral fictive scratch. The AHP amplitude remained decreased immediately following fictive scratch (*D*) and was fully recovered within 10 s of scratch cessation (denoted by *), when compared to control (*B*). Full recovery of AHP amplitude is clearly illustrated by the overlay of the action potentials in the inset. *C* and *E* show an expanded timescale of action potentials evoked by the scratch CPG. AHP amplitude was partially reduced prior to (*C*) scratch and was almost completely absent during scratch (*E*), when compared to control (*B*).

the spike as the baseline would result in a smaller AHP than those measured under control conditions. For this reason, only a qualitative comparison was made of the AHP during control conditions (evoked by ramp or short-duration current pulses) and during the depolarized phase of the SDP. In all 41 cells examined, visual inspection found an obvious reduction in AHP amplitude in motoneurones during fictive scratch and in both spinal intact and acute spinal preparations Figs 2 and 5, respectively. The AHP recovered to control amplitude within seconds following fictive scratch (Fig. 7). Whereas all 41 motoneurones displayed a strong suppression of the AHP, V_{th} was hyperpolarized in only 33. Therefore, there appears to be independent mechanisms responsible for V_{th} hyperpolarization and AHP amplitude reduction.

AHP amplitude reduction is not due to a high conductance state during fictive scratch

A transition to a high conductance state in the motoneurone is a potential explanation for the reduction in AHP amplitude during scratch. To determine whether such a state is present during fictive scratch in the cat, conductance measurements were obtained using brief (5 ms) hyperpolarizing (4–5 nA) current pulses during fictive scratch in motoneurones from a variety of motoneurone pools in one preparation before and after spinalization. The small hyperpolarizing pulse on the current trace in Fig. 5B preceding the pulse used to generate action potentials is an example of the currents used to make conductance measurements. Figure 8 shows the results of conductance measurements

from 10 motoneurones. Values obtained during the depolarized and hyperpolarized phases of rhythmic scratch are shown normalized to values obtained under control conditions. The vertical grey bar separates cells recorded before and after spinal transection at C1. The conductance changes were modest during fictive scratch and in some motoneurones conductance decreased. The mean overall conductance change obtained from pooling measurements from both rhythmic phases of fictive scratch in the 10 motoneurones was an increased conductance of 1.3% with a range of a decrease of 35% to an increase of 34%. Acute spinalization had little effect on motoneurone conductance during scratch. There was no evidence for consistently large increases in motoneurone conductance during the approach (not shown), hyperpolarizing or depolarizing phases of fictive scratch. Therefore, increases in motoneurone conductance are unlikely to be responsible for the large reduction in AHP amplitude during fictive scratch. Rather, it is more likely that fictive scratch involves a suppression of the conductances underlying the AHP. Importantly, this suppression is maintained in acute spinal preparations.

Voltage-dependent amplification of SDPs

The recognition that spinal motoneurones can express intrinsic, voltage-activated, self-sustaining, depolarizing currents (see Heckman *et al.* 2003) has been an important advance in our understanding of how motoneurones are activated during movement. Voltage-dependent amplification of depolarizing drive potentials has been demonstrated during both locomotion and scratch
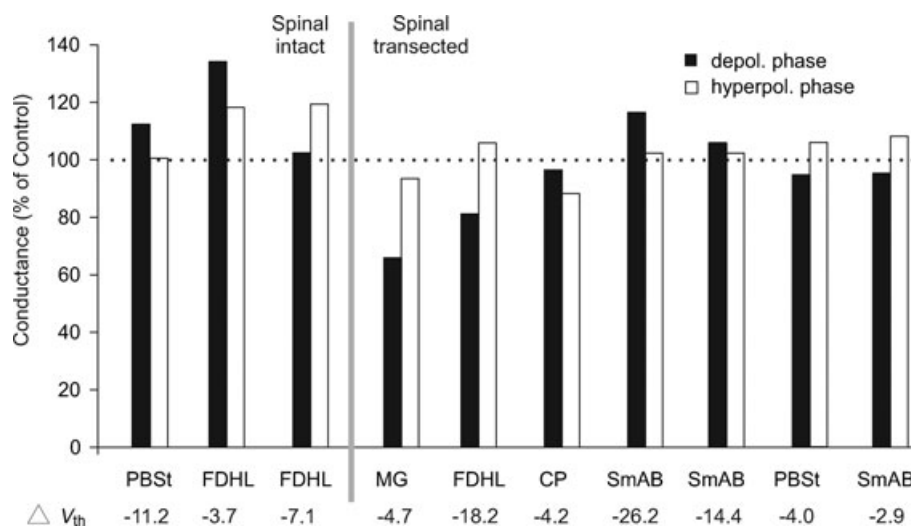

Figure 8. Conductance changes during fictive scratch
Bars represent the average conductance determined for the depolarized (filled bars) and hyperpolarized (open bars) phases of the fictive scratch cycle in a sample of 10 motoneurones. Values are normalized to control (100% as indicated by the horizontal, dashed black line). The narrow grey bar separates the motoneurones in which conductance assessment was done before ($n = 3$) or after spinal transection ($n = 7$). All data are from one cat.

in spinal intact, decerebrate cats (Brownstone *et al.* 1994). The present study sought to determine whether such voltage-activated conductances are also present in spinalized preparations during fictive scratch. If voltage-activated conductances are enabled, then SDP amplitude should increase with intracellular depolarizing current injection and decrease with hyperpolarizing current injection.

The effects of intracellular current injection are shown in Fig. 9 in an acutely spinalized preparation. Triangular-shaped depolarizing currents of 10 nA amplitude were injected into this extensor (Tib) motoneurone in which action potentials had been blocked with QX314 in the microelectrode. The responses to two current injections before and two during fictive scratch are shown. During control conditions, the voltage response in the motoneurone is symmetrical on the ascending and descending portions of the current injection. During fictive scratch, the SDPs are super-imposed on the membrane potential change induced by the current ramp. As the motoneurone is depolarized by the current injection, SDP amplitude increases. This is illustrated by the divergence of the lines bridging the

peaks and troughs of the SDPs in panel *A*. Panel *B* shows the overlay of two SDPs recorded in the absence of current injection, on two at the peak of the second ramp during the fictive scratch. Note the larger SDP that occurs when the motoneurone membrane potential is most depolarized in this acute spinal cat. This example is similar to the effects of current injection reported earlier during fictive scratch in a spinal cord-intact preparation (Brownstone *et al.* 1994). One difficulty in interpreting such results is that SDPs have a hyperpolarizing as well as a depolarizing component (see Perreault 2002). Thus, depolarizing current injection could increase SDP amplitude by activating voltage-dependent excitatory conductances or by increasing the driving potential for the hyperpolarizing portion of the SDP.

Figure 10 shows records from a MG motoneurone in another acutely spinalized preparation at the onset of ipsilateral fictive scratch. There is an initial approach phase indicated by tonic activity in TA, followed by rhythmic alternating activity in flexor and extensor motoneurone pools that continued beyond the period illustrated. During the rhythmic portion of fictive scratch, the motoneurone was hyperpolarized by passing −8 nA of current through
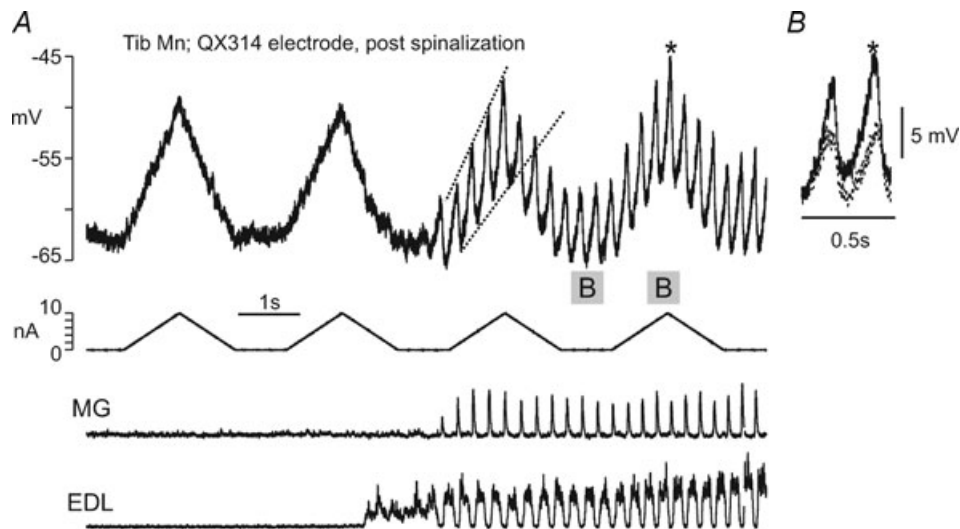

Figure 9. Voltage-dependent amplification of scratch drive potentials in an acutely spinalized preparation
A illustrates the membrane potential recording of a Tib motoneurone (upper trace) in which action potentials were blocked by inclusion of QX314 in the microelectrode. Prior to the onset of fictive scratch, two 10 nA ramps of depolarizing current (middle trace) were delivered which caused ~15 mV depolarizations of the motoneurone membrane potential. After the initiation of fictive scratch indicated by the alternating activity in the MG and EDL ENGs (lower traces) as well as SDPs in the motoneuron, the delivery of the current ramps was repeated. The dashed lines on the first current injection delivered during fictive scratch approximate the peak-to-peak amplitude of the SDPs on the ascending portion of the current ramp. Note that divergence of the slopes of the dashed lines indicates that SDPs occurring at more depolarized membrane potentials were larger than those occuring at more hyperpolarized membrane potentials. On the second current ramp during fictive scratch, the 2 SDPs occurring during no current injection (indicated with the grey box and 'B') are compared to the 2 SDPs occurring during the maximum depolarization induced by the current injection (also indicated with a grey box and 'B'). These SDPs are shown superimposed on an expanded time scale in *B*, aligned at the most hyperpolarized portion of the SDP. The largest SDP (denoted by *) occurred at the most depolarized membrane potential.

the electrode. This hyperpolarization caused an immediate decrease in the amplitude of the SDP that returned to its previous size when the current was switched off. Depolarization of the motoneurone membrane potential by injection of an +8 nA current immediately increased SDP amplitude. The inset panel shows SDP amplitude in the three conditions.

Evidence for voltage-dependent amplification of the SDP similar to the examples in Figs 9 and 10 were seen in motoneurones examined in spinal intact (10/10 motoneurones) and acutely spinalized preparations (19/22 cells). In 18/24 motoneurones (16/22 in spinal transected, 2/2 in spinal intact) hyperpolarizing current injection caused an average decrease of 13.9% in the peak amplitude of the SDP. Our interpretation of the effects of hyperpolarizing currents is that they antagonized the voltage-dependent depolarizations that had already been activated by the scratch CPG. In 15/17 motoneurones (6/7 in spinal transected, 9/10 in

spinal intact) depolarizing current injection induced an average increase of 38.8% in SDP amplitude. The ability of depolarizing currents to further increase SDP amplitude suggests that the scratch-induced activation of voltage-dependent depolarization was only partial in most cases.

Discussion

This report is the first to show that the excitability of lumbar motoneurones is increased during fictive scratch in spinal intact and acutely spinalized preparations. The major findings are that state-dependent enhancements of motoneurone excitability occur during fictive scratch and unexpectedly, these changes persist following acute spinal transection. During ipsilateral scratch in both spinal-intact and spinal-transected preparations there is: (1) a hyperpolarization of V_{th} for action potential initiation during ipsilateral scratch, (2) a decrease in AHP
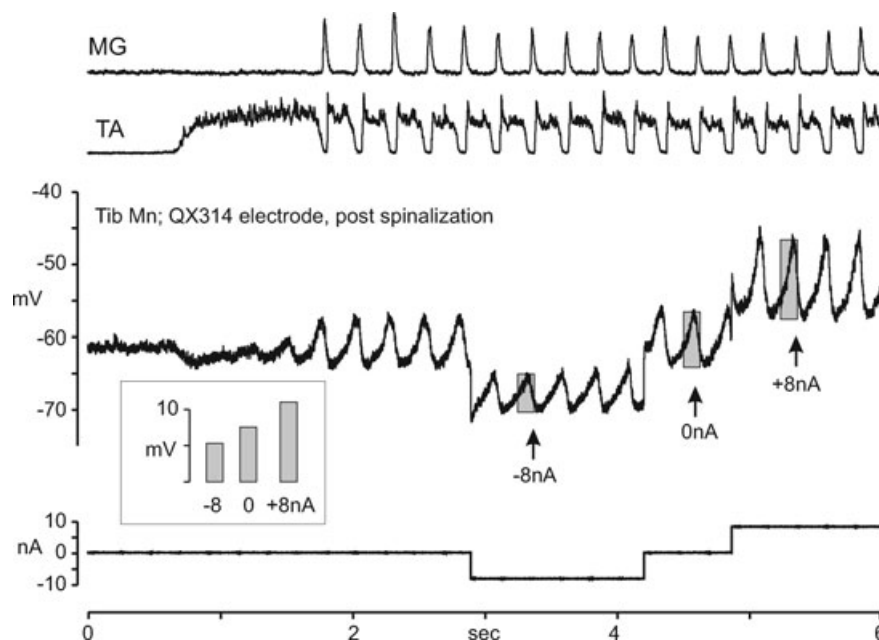

Figure 10. Voltage-dependent amplification of scratch drive potentials can occur spontaneously during fictive scratch in an acutely spinalized preparation
The upper traces show the MG and TA ENGs prior to, and during a bout of ipsilateral scratch in an acutely spinalized preparation. The middle trace shows the membrane potential recording from a Tib motoneurone (same cell as in Fig. 9) in which the action potentials were blocked by including QX314 in the microelectrode. Note the hyperpolarization of the motoneurone occurring during the tonic activity in the TA ENG and which is typical for extensor motoneurones during the approach phase. With the onset of rhythmic scratch and alternating ENG activity, prominent SDPs are evident in the motoneuron. After approximately 5 rhythmic scratch cycles, −8 nA of hyperpolarizing current was delivered to the motoneurone (see current trace at bottom), which was terminated at approximately 4.2 s. At approximately 4.9 s, +8 nA of depolarizing current was delivered. The shaded bars on the membrane potential traces during the −8 nA, 0 nA and +8 nA current periods indicate the peak-to-peak amplitude of the SDP. The inset shows those amplitudes side by side on the same scale and indicate that depolarization of the motoneurone caused the largest SDPs, but also that hyperpolarization of the motoneurone could reduce the amplitude of the SDP compared to those occurring in the absence of current injection. This indicates that the scratch network was able to induce a degree of voltage-dependent amplification of the SDP in the absence of current injection.

amplitude, and (3) a voltage-dependent amplification of SDPs. In contrast to the hyperpolarization in ipsilateral motoneurones, V_{th} is depolarized on the contralateral side in extensors motoneurones active in fictive body weight support.

V_{th} hyperpolarization during fictive scratch shares several features of that found in lumbar motoneurones found during fictive locomotion in spinal cord-intact preparations (Krawitz *et al.* 2001). In both locomotion and scratch, V_{th} hyperpolarization occurs in extensor, flexor and bifunctional motoneurones, and in both high and low rheobase motoneurones. The degree of threshold reduction is similar in fictive scratch and locomotion, (scratch mean: -5.8 mV; locomotion mean: -8.0 mV) and this reduction is present during both the hyperpolarized and depolarized phases of the scratch and locomotor cycles. V_{th} hyperpolarization occurs before any centrally generated firing activity is evoked during both scratch and locomotion. V_{th} reduction was readily evident in extensor motoneurones during the tonically hyperpolarized approach phase in fictive scratch (see Fig. 2). Thus, the modulation of V_{th} is not dependent upon repetitive firing in the motoneurone. Previous modelling work suggests that alterations in the voltage dependency of sodium channels near the axon hillock are a reasonable explanation for threshold lowering without a concomitant change in action potential shape or amplitude during fictive locomotion (Dai *et al.* 2002).

Alterations in V_{th}

Chronic hyperpolarization of motoneurone V_{th} is found following training of the siphon withdrawal reflex in *Aplysia* (Cleary *et al.* 1998) and following 16 weeks of treadmill training in adult rats (Beaumont & Gardiner, 2003). During fictive locomotion there is an immediate, state-dependent and reversible V_{th} hyperpolarization in adult cats (Krawitz *et al.* 2001) and in the *in vitro* neonatal rat brainstem–spinal cord preparation (Gilmore & Fedirchuk, 2004). Present observations during fictive scratch in acute spinal cats show that the rapid onset and recovery of motoneurone V_{th} modulation does not depend upon the integrity of descending influences from the brainstem.

Chronic depolarization of V_{th} has been reported during operant conditioning in monkeys (Carp & Wolpaw, 1994), following decreased motoneurone activity as a result of hindlimb unweighting (Cormery *et al.* 2005) and in chronic spinal cats (Hochman & McCrea, 1994) and rats (Beaumont *et al.* 2004). Acutely, depolarization of motoneurone V_{th} has been reported during trains of action potentials evoked by synaptic input (Kolmodin & Skoglund, 1958) or intracellular current injection (Granit *et al.* 1963) and probably results from an accommodative

process in voltage-gated sodium channels that also leads to decreased firing rates (Schwindt & Crill, 1982). Recent evidence suggests that activation of phosphokinase C is one mechanism by which depolarization of V_{th} can occur in neonatal rat spinal neurones (Dai *et al.* 2009). The present observation that V_{th} changes in the hyperpolarizing direction on the side of the cord engaged in rhythmic scratch and in the depolarizing direction on the contralateral side (Fig. 6) shows that V_{th} is modulated specifically to the motor state.

Suppression of motoneurone afterhyperpolarization

The reduction in motoneurone AHP during both the approach and rhythmic phases of the fictive scratch cycle is similar to that reported during brainstem-evoked fictive locomotion in spinal cord-intact, adult cats (Brownstone *et al.* 1992; Krawitz *et al.* 2001). This is the first study to report the strong suppression of the AHP in spinal cats but similar reductions have been seen during drug-induced locomotion in the spinalized, *in vitro* neonatal rat (Schmidt, 1994). Although a previous study (Brownstone *et al.* 1992) used the action potential V_{th} as a reference point from which to measure AHP amplitude, we now know that this baseline is itself hyperpolarized. Consequently, we chose not to report the magnitude of AHP reduction during scratch in millivolts. It is clear, however, that the AHP is almost completely suppressed in many cases during scratch (present results) and fictive locomotion (Brownstone *et al.* 1992; Krawitz *et al.* 2001).

Although the hyperpolarization of V_{th} could reduce AHP amplitude by causing spikes to be activated closer to the AHP reversal potential, we suggest that this would only be a small factor in AHP reduction during fictive scratch. In the examples presented in Figs 2 and 7, the membrane potentials from which the control and approach phase spikes were evoked lie between -36 and -53 mV. Since these values are considerably more depolarized than the AHP reversal potential of -68 to -95 mV reported in anaesthetized cats (Manuel *et al.* 2005), the change in V_{th} by a few millivolts would not result in large decreases in AHP amplitude. It is noteworthy that the AHP was also suppressed during fictive weight support when both the V_{th} and membrane potential remain depolarized (Fig. 6). Large increases in motoneurone input conductance could potentially decrease AHP amplitude by a passive shunting of the AHP conductances. High conductance states likely to drastically alter AHP amplitude to the extent reported here are not present in decerebrate cats during fictive locomotion (Shefchyk & Jordan 1985; Gosgnach *et al.* 2000), fictive scratch (Perreault, 2002; present results) nor during locomotion in neonatal rat (Schmidt, 1994) or mouse (Endo & Kiehn, 2007) spinal cord preparations. Only modest changes in motoneurone conductance

were found in the present study and importantly, AHP amplitude was reduced during both increases or decreases in motoneurone conductance. The high conductance state reported during scratch in the turtle appears to be a feature of that *in vitro* preparation (Alaburda *et al.* 2005; Berg *et al.* 2007).

We consider a state-dependent suppression of the conductances underlying the AHP to be the most likely explanation for the strong AHP suppression and decreased interspike intervals reported here. Recently Miles *et al.* (2007) demonstrated a reduction in AHP amplitude in mouse motoneurones by activation of cholinergic M_2-type receptors. Moreover, they showed that cholinergic C boutons contacting motoneurones originate from a population of spinal interneurons located near the central canal. It is tempting to speculate that these systems could be engaged by CPGs to reduce AHP amplitude during fictive scratch. The occurrence of AHP suppression in some motoneurones without changes in V_{th} indicates some independence in the mechanisms for these two modes of increased motoneurone excitability during fictive scratch. It is also noteworthy that the AHP suppression reported here during fictive scratch occurs in acutely spinalized preparations. As such, it appears to be a state-dependent change activated from a spinal CPG for scratch.

Intraspinal regulation of motoneurone excitability

Krawitz *et al.* (2001) suggested that a neuromodulatory mechanism may be responsible for V_{th} hyperpolarization during fictive locomotion. Gilmore & Fedirchuk (2004) demonstrated that V_{th} hyperpolarization during locomotor-like patterns evoked by brainstem stimulation in the *in vitro* neonatal rat preparation, could be eliminated by cooling the cervical spinal cord or the addition of a serotonergic antagonist, ketanserin, to the bathing solution. Furthermore, bath application of both 5-HT or NA caused reversible V_{th} hyperpolarization in ventral horn neurones in the isolated *in vitro* neonatal rat spinal cord preparation (Fedirchuk & Dai, 2004; Dai *et al.* 2009). These results suggest that descending monoaminergic pathways might contribute to V_{th} hyperpolarization during fictive locomotion and scratch. The present results in spinal animals do not rule out the possibility that multiple systems can either directly cause changes in motoneurone threshold or activate spinal mechanisms responsible for regulating threshold.

In quiescent decerebrate cat preparations, and in particular in acutely spinalized animals, depolarizing current injection results in a more or less linear depolarization of the membrane potential (Hounsgaard *et al.* 1988; Lee & Heckman, 2000; see Fig. 9). During fictive locomotion and scratch (Brownstone *et al.* 1994; Perreault,

2002) and following acute administration of serotonergic and noradrenergic agonists (see Heckman *et al.* 2003), motoneurone responses to depolarization are amplified by the activation of voltage-dependent excitation described as plateau potentials, PICs or bistability. Voltage-dependent excitation disappears after acute spinalization at the lower thoracic levels (Hounsgaard *et al.* 1988) but may re-emerge in chronic spinal conditions (Eken *et al.* 1989; Bennett *et al.* 2001). Accordingly, we expected little voltage-dependent excitation in the acute, C1 level, spinal transected animals used in the present study. Thus, it was surprising that voltage-dependent excitation was readily evident in acutely spinalized cats during scratch. Since in many cells SDP amplitude decreased with membrane potential hyperpolarization, it appears that voltage-dependent excitation was induced by the scratch pattern or rhythm-generating network and was not a consequence of depolarizing current injection. We suggest that the voltage-dependent enhancement of the SDP results from activation of an unknown intraspinal system regulating motoneurone excitability and that this system is engaged in parallel, or is a part of the CPG for scratch. While we cannot exclude some role for descending mono-aminergic pathways in the voltage-dependent excitation of motoneurones in acute spinal preparations, it seems clear that the state-dependent changes in motoneurone excitability are the direct result of operation of the spinal scratch-generating networks. The extent to which voltage dependency in intact or spinal preparations involves the activation of intrinsic persistent Ca^{2+} or Na^+ inward currents (PICs) in spinal motoneurones or results from receptor-mediated effects, such as that produced by the activation of N-methyl-D-aspartate receptors (Nowak *et al.* 1984), or by activation of metabotropic receptors (Delgado-Lezama *et al.* 1997) remains to be determined.

Increased motoneurone excitability during fictive locomotion and scratch

Rhythmic motor behaviours such as scratch and locomotion require both an appropriate pattern of motoneurone activity and sufficient motoneurone activity to move the limbs and support the body. To this end, the state-dependent decrease in motoneurone V_{th}, the voltage-dependent amplification of SDPs and the reduction in the AHP described here would all act to reduce the magnitude of excitatory current needed from the CPG to recruit and sustain adequate motoneurone firing during fictive scratch. The present results do not, however, fully address the extent to which these changes reduce the amount of CPG-generated synaptic current needed to recruit and sustain motoneurone activity. The minimum ramp current evoking firing in extensor motoneurones in the approach phase of scratch was

reduced by ~36% from control conditions. As this current must overcome the tonic hyperpolarization of extensors during approach, this reduction underestimates the contribution of decreased V_{th} to increased motoneurone excitability. Since the AHP has long been implicated as an important regulator of repetitive firing (see Brownstone, 2006), it is likely that the high firing rates during fictive scratch largely result from the substantial reduction in motoneurone AHP seen. Quantitative estimates of the relative degree to which V_{th} hyperpolarization, AHP reduction and voltage-dependent depolarizations contribute to motoneurone recruitment, repetitive firing and ultimately muscle force generation will require further analysis.

The similarity of experimental conditions in the present and a previous study (Krawitz *et al.* 2001) permit a direct comparison of the V_{th} changes occurring in fictive scratch and locomotion. During scratch the mean V_{th} change in those cells whose thresholds hyperpolarized was -5.8 ± 5.6 mV ($n = 45$, observations in spinal intact and transected combined). This value is not significantly different ($P = 0.08$, t test) than that observed during fictive locomotion (-8.0 ± 5.5 mV, $n = 37$; calculated using the values in Table 1 of Krawitz *et al.* 2001). Extreme examples of threshold hyperpolarization (>20 mV) have been observed during both fictive locomotion and scratch. It is noteworthy, that the incidence of V_{th} hyperpolarization was greater during fictive locomotion (100%) than during fictive scratch (83%).

If increasing the excitability of spinal motoneurones is an integral component of spinally generated rhythmic movements, the existence of multiple and perhaps redundant systems for regulating motoneurone excitability would not be surprising. While it is unlikely that scratch and locomotion are produced by identical spinal organizations, the present results raise the possibility that some of the changes in motoneurone excitability observed during fictive locomotion (Krawitz *et al.* 2001) might also result from operation of intrinsic spinal mechanisms. Thus, there may be both descending (e.g. monoaminergic) and intrapsinal systems that can be readily engaged to alter motoneurone excitability.

Conclusion

The present demonstration of multiple changes in motoneurone properties in acute spinal animals provides the first evidence for the existence of spinal mechanisms that can be quickly engaged and terminated to regulate motoneurone excitability during movements produced by spinal CPGs. The possibility that enhancing such mechanisms could aid in the restoration of function following spinal cord injury underscores the need for further investigation.

References

Alaburda A, Russo R, Macaulay N & Hounsgaard J (2005). Periodic high-conductance states in spinal neurons during scratch-like network activity in adult turtles. *J Neurosci* **25**, 6316–6321.

Beaumont E & Gardiner PF (2003). Endurance training alters the biophysical properties of hindlimb motoneurons in rats. *Muscle Nerve* **27**, 228–236.

Beaumont E, Houle JD, Peterson CA & Gardiner PF (2004). Passive exercise and fetal spinal cord transplant both help to restore motoneuronal properties after spinal cord transection in rats. *Muscle Nerve* **29**, 234–242.

Bennett DJ, Li Y & Siu M (2001). Plateau potentials in sacrocaudal motoneurons of chronic spinal rats recorded *in vitro*. *J Neurophysiol* **86**, 1955–1971.

Berg RW, Alaburda A & Hounsgaard J (2007). Balanced inhibition and excitation drive spike activity in spinal half-centers. *Science* **315**, 390–393.

Brownstone RM (2006). Beginning at the end: repetitive firing properties in the final common pathway. *Prog Neurobiol* **78**, 156–172.

Brownstone RM, Gossard JP & Hultborn H (1994). Voltage-dependent excitation of motoneurones from spinal locomotor centres in the cat. *Exp Brain Res* **102**, 34–44.

Brownstone RM, Jordan LM, Kriellaars DJ, Noga BR & Shefchyk SJ (1992). On the regulation of repetitive firing in lumbar motoneurones during fictive locomotion in the cat. *Exp Brain Res* **90**, 441–455.

Carlson-Khuta P & Smith JL (1990). Scratch Responses in normal cats: hindlimb kinematics and muscle synergies. *J Neurophysiol* **64**, 1653–1667.

Carp JS & Wolpaw JR (1994). Motoneuron plasticity underlying operantly conditioned decrease in primate H-reflex. *J Neurophysiol* **72**, 431–442.

Cleary LJ, Lee WL & Byrne JH (1998). Cellular correlates of long-term sensitization in *Aplysia*. *J Neurosci* **18**, 5988–5998.

Cormery B, Beaumont E, Csukly K & Gardiner P (2005). Hindlimb unweighting for 2 weeks alters physiological properties of rat hindlimb motoneurones. *J Physiol* **568**, 841–850.

Dai Y, Jones KE, Fedirchuk B, McCrea DA & Jordan LM (2002). A modeling study of locomotion-induced hyperpolarization of voltage threshold in cat lumbar motoneurones. *J Physiol* **544**, 521–36.

Dai Y, Jordan LM & Fedirchuk B (2009). Modulation of transient and persistent inward currents by activation of protein kinase C in spinal ventral neurons of the neonatal rat. *J Neurophysiol* **101**, 112–128.

Degtyarenko AM, Simon ES, Norden-Krichmar T & Burke RE (1998). Modulation of oligosynpatic cutaneous and muscle afferent reflex pathways during fictive locomotion and scratching in the cat. *J Neurophysiol* **79**, 447–463.

Delgado-Lezama R, Perrier JF, Nedergaard S, Svirskis G & Hounsgaard J (1997). Metabotropic synaptic regulation of intrinsic response properties of turtle spinal motoneurones. *J Physiol* **504**, 97–102.

Deliagina TG, Feldman AG, Gelfand IM & Orlovsky GN (1975). On the role of central program and afferent inflow in the control of scratching movements in the cat. *Brain Res* **100**, 297–313.

Deliagina TG, Orlovsky GN & Perret C (1981). Efferent activity during fictitious scratch reflex in the cat. *J Neurophysiol* **45**, 595–604.

Domer FR & Feldberg W (1960). Scratching movements and facilitation of the scratch reflex produced by tubocurarine in cats. *J Physiol* **153**, 35–51.

Drummond GB (2009). Reporting ethical matters in *The Journal of Physiology*: standards and advice. *J Physiol* **587**, 713–719.

Eken T, Hultborn H & Kiehn O (1989). Possible functions of transmitter controlled plateau potentials in alpha-motoneurones. *Prog Brain Res* **80**, 257–267.

Endo T & Kiehn O (2007). Conductance measurements of synaptic inputs to mammalian motor neurons during locomotion. *Society for Neuroscience Abstracts* **188.8**.

Fedirchuk B & Dai Y (2004). Monoamines increase the excitability of spinal neurones in the neonatal rat by hyperpolarizing the threshold for action potential production. *J Physiol* **557**, 355–361.

Gilmore J & Fedirchuk B (2004). The excitability of lumbar motoneurones in the neonatal rat is increased by a hyperpolarization of their voltage threshold for activation by descending serotonergic fibers. *J Physiol* **558**, 213–224.

Gosgnach S, Quevedo J, Fedirchuk B & McCrea DA (2000). Depression of group Ia monosynaptic EPSPs in cat hindlimb motoneurones during fictive locomotion. *J Physiol* **526**, 639–652.

Granit R, Kernell D & Shortess GK (1963). Quantitative aspects of repetitive firing of mammalian motoneurones, caused by injected currents. *J Physiol* **168**, 911–931.

Heckman CJ, Lee RH & Brownstone RM (2003). Hyperexcitable dendrites in motoneurons and their neuromodulatory control during motor behavior. *Trends Neurosci* **26**, 688–695.

Hochman S & McCrea DA (1994). Effects of chronic spinalization on ankle extensor motoneurones. II. Motoneuron electrical properties. *J Neurophysiol* **71**, 1468–1479.

Hounsgaard J, Hultborn H, Jespersen B & Kiehn O (1988). Bistability of a-motoneurones in the decerebrate cat and in the acute spinal cat after intravenous 5-hydroxytryptophan. *J Physiol* **405**, 345–367.

Hultborn H, Denton ME, Wienecke J & Nielsen JB (2003). Variable amplification of synaptic input to cat spinal motoneurones by dendritic persistent inward current. *J Physiol* **552**, 945–952.

Jankowska E (1959). Instrumental scratch reflex of the deafferented limb in cats and rats. *Acta Biol Exp* **19**, 233–247.

Kolmodin GM & Skoglund CR (1958). Slow membrane potential changes accompanying excitation and inhibition in spinal moto- and interneurons in the cat during natural activation. *Acta Physiol Scand* **44**, 11–54.

Krawitz S, Fedirchuk B, Dai Y, Jordan LM & McCrea DA (2001). State-dependent hyperpolarization of voltage threshold enhances motoneurone excitability during fictive locomotion in the cat. *J Physiol* **532**, 271–281.

Kuo JJ, Lee RH, Zhang L & Heckman CJ (2006). Essential role of the persistent sodium current in spike initiation during slowly rising inputs in mouse spinal neurones. *J Physiol* **574**, 819–834.

Lafreniere-Roula M & McCrea DA (2005). Deletions of rhythmic motoneuron activity during fictive locomotion and scratch provide clues to the organization of the mammalian central pattern generator. *J Neurophysiol* **94**, 1120–1132.

Lee RH & Heckman CJ (2000). Adjustable amplification of synaptic input in the dendrites of spinal motoneurons *in vivo*. *J Neurosci* **20**, 6734–6740.

Manuel M, Meunier C, Donnet M & Zytnicki D (2005). How much afterhyperpolarization conductance is recruited by an action potential? A dynamic-clamp study in cat lumbar motoneurones. *J Neurosci* **25**, 8917–8923.

Miles GB, Hartley R, Todd AJ & Brownstone RM (2007). Spinal cholinergic interneurons regulate the excitability of motoneurons during locomotion. *Proc Natl Acad Sci USA* **104**, 2448–2453.

Nowak L, Bregestovski P, Ascher P, Herbet A & Prochiantz A (1984). Magnesium gates glutamate-activated channels in mouse central neurones. *Nature* **307**, 462–465.

Perreault MC (2002). Motoneurons have different membrane resistance during fictive scratching and weight support. *J Neurosci* **22**, 8259–8265.

Perreault MC, Enriquez-Denton M & Hultborn H (1999). Proprioceptive control of extensor activity during fictive scratching and weight support compared to fictive locomotion. *J Neurosci* **19**, 10966–10976.

Schmidt BJ (1994). Afterhyperpolarization modulation in lumbar motoneurons during locomotor-like rhythmic activity in the neonatal rat spinal cord *in vitro*. *Exp Brain Res* **99**, 214–222.

Schwindt PC & Crill WE (1982). Factors influencing motoneuron rhythmic firing: results from a voltage-clamp study. *J Neurophysiol* **48**, 875–890.

Shefchyk SJ & Jordan LM (1985). Motoneuron input-resistance changes during fictive locomotion produced by stimulation of the mesencephalic locomotor region. *J Neurophysiol* **54**, 1101–1108.

Sherrington CS (1906). *The Integrative Action of the Nervous System*. 1947 edn. Cambridge University Press.

Sherrington CS (1910). Notes on the scratch-reflex of the cat. *Exp Physiol* **3**, 213–220.

Zengel JE, Reid SA, Sypert GW & Muson JB (1985). Membrane electrical properties and prediction of motor-unit type of medial gastrocnemius motoneurons in the cat. *J Neurophysiol* **53**, 1323–1344.

Author contributions

Acknowledgements